AIP | Journal of Applied Physics

B segregation to grain boundaries and diffusion in polycrystalline Si with flash annealing

S. Jin, K. S. Jones, M. E. Law, and R. Camillo-Castillo

Citation: J. Appl. Phys. **111**, 044508 (2012); doi: 10.1063/1.3688246
View online: http://dx.doi.org/10.1063/1.3688246
View Table of Contents: http://jap.aip.org/resource/1/JAPIAU/v111/i4
Published by the American Institute of Physics.

B segregation to grain boundaries and diffusion in polycrystalline Si with flash annealing

S. Jin,[1,a)] K. S. Jones,[1] M. E. Law,[2] and R. Camillo-Castillo[3]
[1]*Department of Materials Science and Engineering, University of Florida, Gainesville, Florida 32611-6400, USA*
[2]*Department of Electrical Engineering, University of Florida, Gainesville, Florida 32611-6400, USA*
[3]*IBM Semiconductor Research and Development Center, Essex Junction, Vermont 05452, USA*

(Received 22 November 2011; accepted 26 January 2012; published online 24 February 2012)

Three-dimensional atom probe tomography was used to characterize the segregation of B dopant atoms to grain boundaries in polycrystalline Si after flash-assisted rapid thermal annealing. Tomographic reconstructions allowed direct measurement of segregation coefficients, which were found to be greater at lower flash temperatures with thermal budgets that limit grain growth. Hall measurements confirmed the deactivation of B at the grain boundaries, while secondary ion mass spectrometry was used to measure B diffusion in the film. Experimental parameters were then simulated in a diffusion model which accurately predicts the diffusion of B in polycrystalline Si at flash temperatures of 1150 °C, 1250 °C, and 1350 °C, as well as with conventional rapid thermal annealing. © *2012 American Institute of Physics*. [http://dx.doi.org/10.1063/1.3688246]

I. INTRODUCTION

Polycrystalline Si, or poly-Si, has many applications in the field of microelectronic devices, from conventional field-effect transistors,[1] to heterojunction bipolar transistors,[2] and photovoltaics.[3] Due to the ever-shrinking feature sizes in transistors, innovations in annealing beyond conventional rapid thermal processing are necessary to limit diffusion and increase activation of dopants.[4] In particular, flash annealing allows low thermal budgets with high temperatures and very short time scales on the order of 1 ms.[5] The combination of high B concentration with low thermal budgets presents an ideal environment for investigating B segregation to the grain boundaries in poly-Si. The degree of segregation can have a profound effect on B diffusion due to the significantly enhanced diffusivity of impurities within grain boundaries. Therefore, it is important to understand the effect of millisecond annealing on B doped poly-Si films.

Three-dimensional atom probe tomography (APT) allows direct analysis of dopant segregation to grain boundaries and other crystalline defects.[6–8] In fact, the technique has already been employed to demonstrate segregation of As and P to grain boundaries in a polysilicon gate electrode.[9] However, there have been conflicting reports as to the segregation of B to grain boundaries. Inoue *et al*. has shown that it does not segregate[9] while atom probe measurements from Thompson *et al*. show significant segregation[10] at grain boundary triple points. Even prior to 3D APT, B segregation to grain boundaries was debatable. Activation and deactivation with cyclical annealing was seen for As doped poly-Si, but not for B for concentrations below solid solubility.[11] On the other hand, it has also been reported that at very high concentrations (>2 at %) B formed precipitates at the grain boundaries of poly-Si.[12] In this work, a weak but detectable segregation of B to the grain boundaries is reported using 3D APT. Grain growth was found to significantly reduce the amount of segregated B due to the reduction in grain boundary surface area. Values obtained from the experimental data were applied to a poly-Si diffusion model,[13,14] which accurately predicts diffusion of B in flash annealed poly-Si. Hall measurements suggest that the segregated B is electrically inactive.

II. EXPERIMENTAL

120 nm poly-Si films were deposited by low-pressure chemical vapor deposition on bulk Si wafers with ~12 nm of SiO_2. B doping was done *in situ* to a total dose of 2.5×10^{15} cm^{-2}, which amounts to a peak concentration below the solid solubility level[15] of 3.0×10^{20} cm^{-3} for anneal temperatures above 1250 °C. Additionally, some samples were further doped by ion implantation, beginning with a preamorphizing implant using Ge^+ at 40 keV to a dose of 5.0×10^{14} cm^{-2}, followed by an additional B^+ implant at 10 keV to bring the total dose of the film to 4.9×10^{15} cm^{-2} as measured by SIMS. The preamorphizing implant produced a 60 nm-thick continuous amorphous layer. At this dose, the peak B concentration remains above the solid solubility limit at all flash temperatures. Initial doping profiles are displayed in Fig. 1.

Annealing was carried out for both B doses using an impulse rapid thermal anneal (iRTP) at a ramp rate of 150 °C/s to a pre-flash temperature of 850 °C, and then subsequently flash annealed to 1150 °C, 1250 °C, and 1350 °C with a pulse duration of 1 ms. For comparison, samples were also annealed using a conventional rapid thermal anneal (RTA) at 988 °C for 5 s.

Specimens were prepared for 3D APT using an FEI Strata DB235 dual-beam focused-ion beam (FIB) using the liftout method.[16] The samples were first coated with 50 nm Ni by sputter deposition to act as a sacrificial buffer layer to Ga beam damage from the FIB. Annular milling produced atom

a)Author to whom correspondence should be addressed. Electronic mail: sidan@ufl.edu.

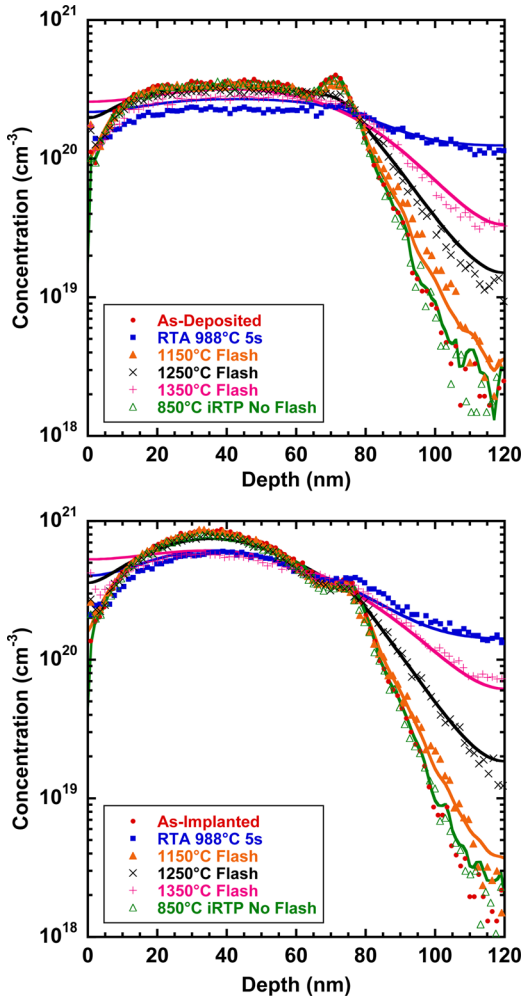

FIG. 1. (Color online) B concentration profiles for *in situ* doped and additionally B implanted poly-Si films with various annealing conditions. Solid lines represent simulated profiles.

probe tips with a radius of curvature of less than 50 nm. 3D APT was carried out using an Imago LEAP 3000X-Si system equipped with a 532 nm green pulsed laser. The laser pulse energy was set to 1.0 nJ and specimen temperature cooled to 60 K. The laser pulse rate was set to 100 kHz with an evaporation rate of 0.5%. Typical datasets ranged between 5–10 $\times$ 10^6 ions. Concentration profiles for the films were measured using secondary ion mass spectrometry (SIMS), with a Cs^+ primary beam at 3 keV.

III. RESULTS AND DISCUSSION

3D APT reconstructions revealed the presence of local areas of higher concentration than the bulk. By using the volume render function in the reconstruction software, local concentrations less than 1 at % within one standard deviation can be filtered out. This was done in order to aid in locating areas of relatively higher B concentrations. The volume render is illustrated in Fig. 2, revealing the segregation of B to the grain boundaries. This grain boundary measures 42 nm, which is the average grain size for this sample. The sample was annealed at 988 °C for 5 s. In Fig. 3, a one-dimensional concentration profile across the grain boundary is compared with a profile within the grain. This was done by extracting a concentration profile

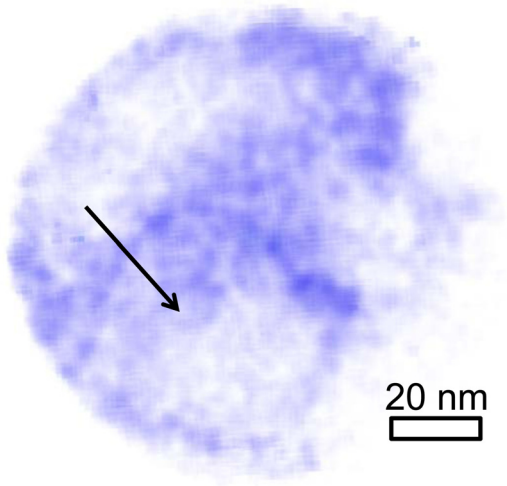

FIG. 2. (Color online) 3D atom probe reconstruction using volume rendering, with local concentrations below 1 at % filtered out to highlight the grain. Only B atoms are shown. The arrow depicts where the 1-D concentration profile was extracted.

along the z-axis of a 10 nm $\times$ 10 nm $\times$ 40 nm data pipe across the grain boundary in the reconstruction. A second data pipe of the same dimensions was inserted into an area within a grain. Segregation of B to the grain boundary is clearly evident.

From Eq. (1), the ratio of the peak concentration within the boundary to the average concentration within the grain represents the local segregation coefficient, m_{seg}. Because this represents only the segregation of B to a single grain boundary, an estimate must be made to account for the total amount of segregated B in the film. Assuming spherical grains with a diameter L, the volume fraction term, X_{gb}, in Eq. (2) is estimated using a grain boundary thickness, t_{gb}, of $2b$, where b is the lattice constant,[17] multipled by $(3/L)$, the surface-area-to-volume ratio.[18] This calculation assumes that adjacent grains share a single grain boundary. Multiplying the local segregation coefficient, m_{seg} by X_{gb} gives p_{seg}, the segregation coefficient used in prior models for diffusion of

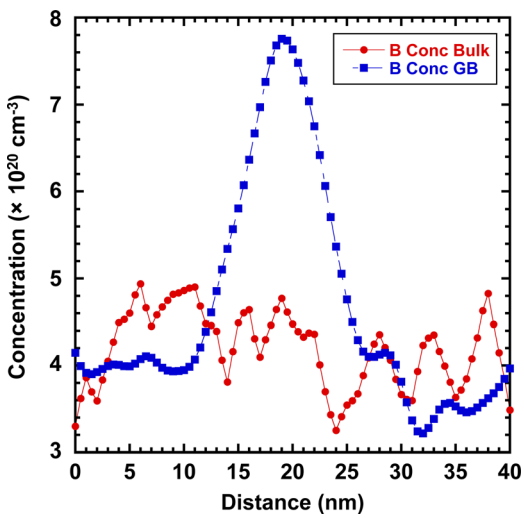

FIG. 3. (Color online) 1-D concentration profile across the grain boundary depicted in Fig. 2 (squares). For reference, the bulk concentration within the grain is also plotted (circles).

dopants in polysilicon.[13,14,19] The highest local segregation coefficient was measured to be only about 3.0 at the lowest flash temperatures. Higher temperatures and longer anneals significantly reduce the coefficient of locally segregated B at a single grain to about 1.5,

$$m_{seg} = \frac{C_B^{gb}}{C_B^g}, \tag{1}$$

$$X_{gb} = t_{gb}\left(\frac{3}{L}\right), \tag{2}$$

$$p_{seg} = \frac{A}{L(t)}\frac{Q_{Si}}{N_{Si}}\exp\left(\frac{G_A}{kT}\right) = X_{gb}m_{seg}. \tag{3}$$

The equation for p_{seg} used in the PEPPER (Ref. 13) diffusion model given by Eq. (3) has been used as the basis for the experimental results obtained from 3D APT. Q_{Si} is the density of segregation sites available on a grain boundary, previously calculated[11] to be 2.64×10^{15} cm^{-2} for spherical grains, and N_{Si} is the density of silicon, 5.0×10^{22} cm^{-3}.

Values for p_{seg} are plotted versus flash temperature for both the implanted and *in situ* doped samples in Fig. 4. The pre-exponential A was calculated to be 0.8 ± 0.06, with a heat of segregation, G_A, of 0.36 ± 0.2 eV. For comparison,[11] previous values for the pre-exponential published for As and P are 3.02 and 2.46, respectively, and both share a heat of segregation of 0.456 eV at a concentration of 2.0×10^{19} cm^{-3}. For B, there is significantly less segregation to the grain boundaries when compared to As or P.[11]

The term $L(t)$ in Eq. (3) represents the grain diameter. Grain growth mechanisms in B doped poly-Si have been well-studied[19,20] for furnace anneals, and so the work here is an extension of their model to the millisecond annealing regime. Grain size measurements were taken using plan-view transmission electron microscopy, and fit to a model for grain growth[19] with flash annealing conditions. This is given by Eq. (4), where L_0 is the initial grain diameter (19 nm), b is the lattice constant, λ is the grain boundary energy, and t is the duration of the anneal ($t = 0.001$ s for flash anneals). Assuming a grain boundary energy[17,19] of 1.0 J/m^2, the pre-exponential A is calculated to be 5.0×10^6, and the activation energy for grain growth was found to be 4.7 ± 0.1 eV, which is the same as the activation energy reported for Si self-diffusion.[19,21] It is important to note that the grain boundary energy, λ, will decrease as the grain size approaches the film thickness,[19] representing a change in interfacial energy with the underlying oxide. This is modeled using Eq. (5), where λ_0 represents no oxide interaction, η is the surface area to volume ratio ($3/L$), l is the film thickness, and h is a constant experimentally determined to be 6,

$$L = \left[L_0^2 + \frac{Ab^2}{kT}\lambda D_{Si} t\right]^{1/2}, \tag{4}$$

$$\lambda = \frac{\lambda_0}{1 + h\frac{2}{\eta l}}. \tag{5}$$

Based on previous reports,[19,22] no effect on microstructure was expected due to the additional Ge^+ pre-amorphization and B^+ implant, and indeed no there was not a significant effect. There was also no effect seen with regard to transient enhanced diffusion,[23] which was not expected for a number of reasons. First, even at the lowest flash temperature of 1150 °C, the enhancement factor of C_i/C_i^* in transient enhanced diffusion approaches unity due to the high concentration of intrinsic interstitials for crystalline silicon,[21] although it is not known how a polycrystalline structure might effect this value. Secondly, it is likely that the significantly greater diffusivity via the grain boundaries overwhelmingly dominates as the mechanism for diffusion.

Diffusion of B in poly-Si was modeled using the Florida Object Oriented Process Simulator[24] (FLOOPS) using equations based on the PEPPER model,[13] which separates the diffusivity of the impurity into two components; diffusivity within the grain (6) and diffusivity along the grain boundary (7). The two differential equations are coupled with a kinetic reaction term, which drives $C^{gb}/C^g = p_{seg}$ at steady state. τ is a constant that represents the rate of segregation. The extrinsic diffusivity within the grain comes from Fair's model[25] for B diffusivity (8), which accounts for the enhanced diffusivity with higher B concentration in the films[25] by way of an enhancement factor of (p/n_i), where p is the hole density from Hall effect measurements and n_i is the intrinsic hole concentration[26] at the anneal temperature. The diffusivity along the grain boundary (9) was determined previously,[27]

$$\frac{\partial C_B^g}{\partial t} = D_B^g\frac{\partial^2 C_B^g}{\partial x^2} + \tau^{-1}(C_B^g p_{seg} - C_B^{gb}), \tag{6}$$

$$\frac{\partial C_B^{gb}}{\partial t} = D_B^{gb}\frac{\partial^2 C_B^{gb}}{\partial x^2} - \tau^{-1}(C_B^g p_{seg} - C_B^{gb}), \tag{7}$$

$$D_B^g = 0.037\exp\left(\frac{-3.46}{kT}\right) + \left(\frac{p}{n_i}\right)0.76\exp\left(\frac{-3.46}{kT}\right), \tag{8}$$

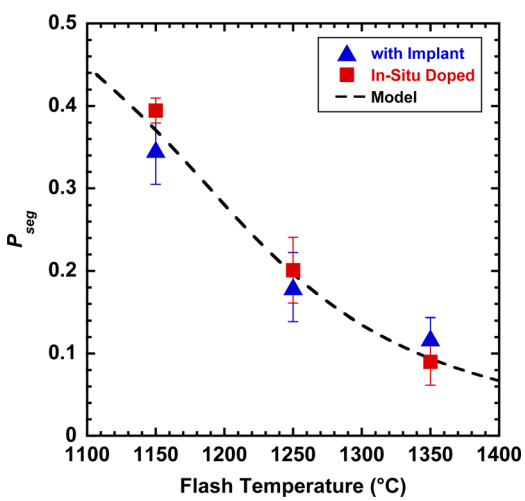

FIG. 4. (Color online) p_{seg} values from atom probe tomography are plotted for both the *in situ* doped (squares) and implanted (triangles) samples. The dotted line represents the values generated from the model.

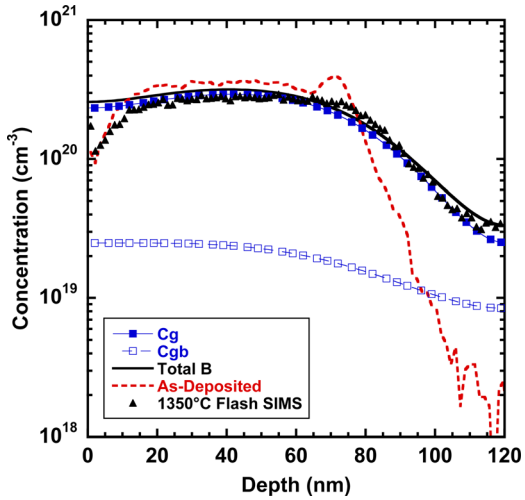

FIG. 5. (Color online) An example of the diffusion model for a 1350 °C flash anneal on an *in situ* doped sample.

$$D_B^{gb} = 0.012 \exp\left(\frac{-2.0}{kT}\right). \quad (9)$$

Using these equations, the model for B diffusion in poly-Si is overlaid with the respective SIMS profiles in Fig. 1. For flash anneals, the time-temperature profiles are simulated based off of the temperature profiles generated from measuring the top-surface of the wafer using an optical pyrometer. The wafers experienced a 150 °C/s ramp rate from 20 °C to the pre-flash temperature of 850 °C, followed by the flash, which is represented using a 10^6 °C/s ramp rate and dwell time of 1 ms at the peak flash temperature. The cooling is modeled at -1×10^5 °C/s, -7×10^4 °C/s, and -4×10^4 °C/s from the peak flash temperatures of 1150 °C, 1250 °C, and 1350 °C, respectively. Following the flash, the wafer surface temperatures rise to 900 °C, 920 °C, and 950 °C, for the 1150 °C, 1250 °C, and 1350 °C flash anneals, respectively. The rise in surface temperature is more pronounced for higher flash temperatures. Finally, the wafers cool at 100 °C/s to room temperature.

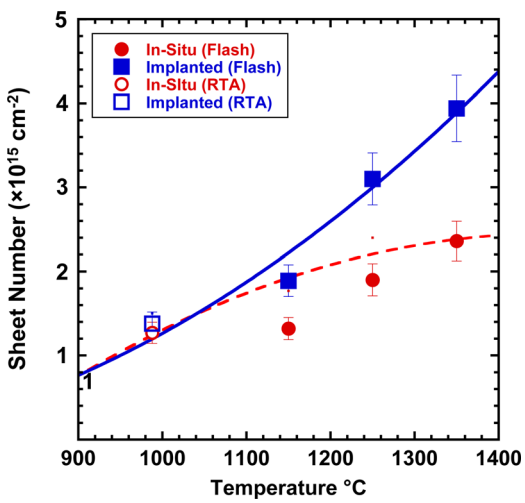

FIG. 6. (Color online) Sheet number values from Hall measurements for *in situ* doped and implanted samples annealed using flash and conventional RTA. Dashed and solid lines represent the theoretical activation for *in situ* doped and implanted samples, respectively.

TABLE I. Comparison between predicted active dose and Hall sheet number for *in situ* B doped poly-Si at various flash temperatures.

T °C	Predicted active dose (cm^{-2})	Hall sheet number (cm^{-2})
1150	1.5×10^{15}	1.32×10^{15}
1250	2.0×10^{15}	1.90×10^{15}
1350	2.3×10^{15}	2.36×10^{15}

Similarly, temperature profiles for the 850 °C iRTP spike and 988 °C RTA anneal are modeled using 150 °C/s and 75 °C/s ramp rates, respectively, and both cooled at 100 °C/s.

The constant τ^{-1} representing the rate of segregation has been extracted from the model iteratively by fitting to the diffusion profiles. It is shown to have Arrhenius behavior, given in Eq. (10), and was found to be independent of anneal time,

$$\tau^{-1} = 6.1 \times 10^{22} \exp\left(\frac{-5.8}{kT}\right). \quad (10)$$

As an example, Fig. 5 depicts the separation of the two concentration profiles, C^g and C^{gb} as the dopant diffuses through the layer for the 1350 °C flash anneal of the *in situ* doped sample. At this annealing condition, all of the dopant is below the solid solubility limit for B in crystalline Si.[15] Hall measurement for this sample gives a sheet number of 2.36×10^{15} cm^{-2}, which agrees well with the integrated area under the curve for C^g (2.35×10^{15} cm^{-2}) in Fig. 5.

Hall measurements also revealed that the active dose in the implanted case matches well with the theoretical solubility of B in crystalline Si.[15] However, for the *in situ* doped sample, activation does not reach the theoretical value until 1350 °C flash temperatures. These results are shown in Fig. 6 with comparisons to theoretical activation levels based on solubility data.[15] Because the *in situ* doped sample had a lower total dose, segregation to the grain boundary accounted for a noticeable difference from expected activation values. For the additionally implanted samples, the concentration of segregated B to the grain boundary had reached saturation due to the high dose. This is verified in Table I, where the predicted active dose for the *in situ* doped samples, calculated by assuming the segregated B is inactive, matches closely with the sheet number values from Hall measurements. The predicted active dose equals the total dose minus the segregated B dose, which is calculated by multiplying the total dose by p_{seg}.

IV. CONCLUSION

B segregation to grain boundaries was imaged directly using 3D atom probe tomography, proving that it does in fact segregate under these concentrations and annealing conditions. The measured segregation coefficients were applied to a diffusion model to accurately predict the diffusion of B in poly-Si. Given solubility constraints, the model reasonably predicts the expected activation levels of the dopant by assuming individual crystallites have the properties of bulk single-crystalline Si. From this, it can be inferred that the B segregated to the grain boundaries is not electrically active.

The model presented here for B segregation to the grain boundary can also be applied to traditional thermal processing. The results are able to support the conclusions reported previously where segregation was not detected, while also demonstrating that under flash annealing conditions with heavy doping, B segregates moderately to grain boundaries in poly-Si. The highest local segregation coefficient measured here is only about 3.0 at the lowest flash temperature of 1150 °C, and drops to as low as 1.5 with greater thermal budget. It is shown that longer duration anneals and high temperature anneals, both conditions that promote grain growth and solubility, respectively, lead to a significant reduction in the segregation of B to the grain boundary.

ACKNOWLEDGMENTS

The authors would like to acknowledge IBM corporation for their collaboration in this project, with specific mention to Paul Ronsheim and Michael Hatzistergos for atom probe assistance, as well as Mikhail Klimov at the University of Central Florida for SIMS analysis, and the Nanofabrication Research Facility (NRF) and Major Analytical and Instrumentation Center (MAIC) at the University of Florida.

[1]F. Faggin and T. Klein, Solid-State Electron. **13**, 1125 (1970).
[2]H. Rücker, B. Heinemann, R. Barth, D. Knoll, P. Schley, R. Scholz, B. Tillack, and W. Winkler, Mater. Sci. Semicond. Process. **8**, 279 (2005).
[3]L. Carnel, I. Gordon, D. Van Gestel, G. Beaucarne, and J. Poortmans, Thin Solid Films **516**, 6839 (2008).
[4]D. Bolze, B. Heinemann, J. Gelpey, S. McCoy, and W. Lerch, presented at the 17th International Conference on Advanced Thermal Processing of Semiconductors, Albany, NY, 2009.
[5]T. Gebel, M. Voelskow, W. Skorupa, G. Mannino, V. Privitera, F. Priolo, E. Napolitani, and A. Carnera, Nucl. Instrum. Methods B **186**, 287 (2002).
[6]S. Duguay, Appl. Phys. Lett. **97**, 242104 (2010).
[7]M. L. Taheri, J. T. Sebastian, B. W. Reed, D. N. Seidman, and A. D. Rollett, Ultramicroscopy **110**, 278 (2010).
[8]K. Thompson, P. L. Flaitz, P. Ronsheim, D. J. Larson, and T. F. Kelly, Science **317**, 1370 (2007).
[9]K. Inoue, F. Yano, A. Nishida, H. Takamizawa, T. Tsunomura, Y. Nagai, and M. Hasegawa, Appl. Phys. Lett. **95**, 043502 (2009).
[10]K. Thompson, J. H. Bunton, T. F. Kelly, and D. J. Larson, J. Vac. Sci. Technol. B **24**, 421 (2006).
[11]M. Mandurah, J. Appl. Phys. **51**, 5755 (1980).
[12]G. L. Pearson and J. Bardeen, Phys. Rev. **75**, 865 (1949).
[13]B. J. Mulvaney, W. B. Richardson, and T. L. Crandle, IEEE Trans. Comput.-Aided Des. **8**, 336 (1989).
[14]L. Mei and R. W. Dutton, IEEE Trans. Electron Devices **29**, 1726 (1982).
[15]V. E. Borisenko and S. G. Yudin, Phys. Status Solidi A **101**, 123 (1987).
[16]K. Thompson, D. Lawrence, D. J. Larson, J. D. Olson, T. F. Kelly, and B. Gorman, Ultramicroscopy **107**, 131 (2007).
[17]S. P. Chen, J. D. Kress, A. F. Voter, and R. C. Albers, presented at the 4th International Symposium on Process Physics and Modeling in Semiconductor Technology, 1996.
[18]W. Hosford, *Materials Science: An Intermediate Text*. (Cambridge University Press, Cambridge, 2007).
[19]L. Mei, M. Rivier, Y. Kwark, and R. W. Dutton, J. Electrochem. Soc. **129**, 1791 (1982).
[20]S. Kalainathan, R. Dhanasekaran, and P. Ramasamy, J. Electron. Mater. **19**, 1135 (1990).
[21]A. Ural, P. B. Griffin, and J. D. Plummer, Phys. Rev. Lett. **83**, 3454 (1999).
[22]Y. Komem and I. W. Hall, J. Appl. Phys. **52**, 6655 (1981).
[23]C. Bonafos, M. Omri, B. de Mauduit, G. BenAssayag, A. Claverie, D. Alquier, A. Martinez, and D. Mathiot, J. Appl. Phys. **82**, 2855 (1997).
[24]M. E. Law and S. M. Cea, Comput. Mater. Sci. **12**, 289 (1998).
[25]R. B. Fair and P. N. Pappas, J. Electrochem. Soc. **122**, 1241 (1975).
[26]C. D. Thurmond, J. Electrochem. Soc. **122**, 1133 (1975).
[27]S. Nedelec, D. Mathiot, and M. Gauneau, presented at the Solid State Device Research Conference, 1996. ESSDERC '96. Proceedings of the 26th European, 1996.